

# RECENT ( $\vec{\gamma}$ ,NN) RESULTS AND FUTURE PLANS

I.J.D. MACGREGOR

*Department of Physics & Astronomy, University of Glasgow, Scotland*

FOR THE PIP/TOF GROUP OF THE MAINZ A2 COLLABORATION

This paper reports on:

1. Recent  $^{12}\text{C}(\vec{\gamma},\text{pn})$  and  $^{12}\text{C}(\vec{\gamma},\text{pp})$  measurements in the  $\Delta$ -resonance region;
2. A proposed experiment to measure Short Range Effects in the  $^{12}\text{C}(\gamma,\text{NN})$  reaction, above the  $\Delta$ -resonance, using detectors close to the photon beamline.

## 1 $^{12}\text{C}(\vec{\gamma},\text{pn})$ and $^{12}\text{C}(\vec{\gamma},\text{pp})$ in the $\Delta$ -Resonance Region

### 1.1 Introduction

Photon asymmetries ( $\Sigma$ ) and cross sections for reactions in which the reaction plane is parallel ( $\sigma_{\parallel}$ ) or perpendicular ( $\sigma_{\perp}$ ) to the incident photon polarisation direction have been measured for the  $^{12}\text{C}(\vec{\gamma},\text{pp})$  and  $(\vec{\gamma},\text{pn})$  reactions for photon energies 170-350 MeV<sup>1,2</sup>. These measurements provide access to observables which are sensitive to the details of the basic interaction<sup>3,4,5</sup> and which can only be measured with polarised photons. The photon asymmetry, defined by  $\Sigma = \frac{\sigma_{\parallel} - \sigma_{\perp}}{\sigma_{\parallel} + \sigma_{\perp}}$ , emphasises the differences between  $\sigma_{\parallel}$  and  $\sigma_{\perp}$  and is insensitive to the similarities.

The ( $\vec{\gamma}$ ,NN) reactions in nuclei are dependent on the meson exchange currents (MEC) and short range correlations (SRC) which contribute to the transverse structure functions  $W_T = W^{xx} + W^{yy}$  and  $W_{TT} = W^{xx} - W^{yy}$ . The unpolarised cross section is proportional to  $W_T$  whereas the photon asymmetry can access the differences between  $W^{xx}$  and  $W^{yy}$  contained in  $W_{TT}$  through the relation  $\Sigma = -\frac{W_{TT}}{W_T}$ .  $W_{TT}$  is particularly sensitive to spin variables in the nuclear currents and also to interference between the contributing currents<sup>4</sup>. Measurements of polarisation observables therefore provide stringent and sensitive tests of models of two-nucleon photoemission reactions.

The present experiments aimed to investigate the  $^{12}\text{C}(\vec{\gamma},\text{pn})$  and  $(\vec{\gamma},\text{pp})$  reactions in the  $\Delta$ -resonance region with reasonable statistical accuracy, kinematic coverage matched to the direct two-nucleon emission process and sufficiently good missing energy resolution ( $\Delta E_m$ ) to separate events in which nucleon pairs are emitted from (1p)<sup>2</sup> and (1p)(1s) orbitals.

## 1.2 Experiment

The experiment was carried out using the Glasgow tagged photon spectrometer<sup>6</sup> at the Mainz 855 MeV electron accelerator MAMI<sup>7</sup>. A 100  $\mu\text{m}$  thick low-mosaic diamond radiator was used to produce coherent bremsstrahlung and the polarisation  $P$  of the photon beam was calculated using a Monte Carlo code<sup>8</sup> incorporating both coherent and incoherent bremsstrahlung processes. Three separate measurements, with different diamond orientations, were used to cover the photon energy range 170-350 MeV. The polarised photons were collimated by a 3mm diameter collimator, 2m downstream of the diamond radiator, before reaching the 0.5g/cm<sup>2</sup> graphite target at 30° to the photon beam line.

Protons were detected in PiP<sup>9</sup>, a  $\sim 1$  sr solid angle plastic scintillation hodoscope covering polar angles from 50° to 130° and azimuthal angles of  $\pm 22^\circ$ . The energy acceptance of PiP was from 31 MeV to 330 MeV. Efficiency losses for protons which undergo inelastic reactions in the scintillator material were corrected using a Monte Carlo simulation.

Correlated nucleons were detected in TOF<sup>10</sup>, an array of plastic scintillator detectors used to measure particle energies by the time-of-flight technique. The TOF stands used covered polar angles 24°–38°, 44°–58°, 62°–81°, and 90°–110° at distances of 7.1m, 7.1m, 5.1m and 4.7m respectively, on the opposite side of the photon beam from PiP. Two half-rings of thin scintillators were used to distinguish charged and neutral particles on the TOF side. The  $E_m$  resolution of the experiment was estimated to be  $\sim 8$  MeV from the width of the  ${}^2\text{H}(\gamma, \text{pn}) E_m$  peak obtained from calibration data.

The tagging efficiency ( $\epsilon_\gamma$ ), the fraction of tagged photons which pass through the tagger collimator, depends on the angular distribution of the coherent bremsstrahlung radiation and hence has a strong photon energy dependence. The maximum  $\epsilon_\gamma$ , measured at the top of the [022] coherent bremsstrahlung peak, was  $\epsilon_\gamma^{max} \sim 60\%$  for the lowest photon energy setting. For the two higher photon energy settings it was  $\epsilon_\gamma^{max} \sim 54\%$  and  $\epsilon_\gamma^{max} \sim 50\%$ .

The cross sections presented are differential in the solid angles of the two detected particles and in the momenta of the protons detected in PiP. The TOF detectors were divided into four solid angle bins. PiP solid angle bins were selected by accepting protons within  $\pm 10^\circ$  of the mean proton polar angle  $\bar{\theta}_p$  conjugate to the centre of each TOF bin. This ensured that the cross sections sampled the peak of the  $(\gamma, \text{NN})$  angular correlation. The proton momentum acceptance was determined by the PiP low energy threshold and an upper limit which was determined by the reaction kinematics<sup>2,11</sup>.

The azimuthal angle of the reaction plane was taken from an “average” of the azimuthal angles of the two emitted nucleons. A cut of  $\pm 13.5^\circ$  was placed on this angle for events contributing to  $\sigma_{\parallel}$  or  $\sigma_{\perp}$  to ensure a uniform azimuthal acceptance, independent of polar angles. A geometrical correction factor ( $\sim 4\%$ )<sup>1</sup> was applied

to to account for the small reduction in  $\Sigma$  produced when  $\sigma_{\parallel}$  and  $\sigma_{\perp}$  are averaged over these finite azimuthal acceptances.

### 1.3 Calculations

The data are compared with predictions of a direct two-nucleon knockout model developed by the Gent theory group<sup>5</sup>. The model calculates cross sections and asymmetries in an unfactorised distorted wave treatment of the interaction. It includes pion exchange and  $\Delta$ -isobar currents and incorporates short-range interactions using a central correlation obtained from a G-matrix calculation by Gearhart and Dickhoff<sup>12</sup>.

The calculations used a Monte Carlo technique<sup>11</sup> to average over the acceptance of the experimental detectors. This is necessary since significant variations in cross section can occur within relatively small angular bins and cross sections evaluated for “central” kinematic conditions for a particular bin can be significantly different from the average over that bin. In particular there is a strong variation in cross sections with initial pair momentum  $\mathbf{P}$  which results in average cross sections being significantly weaker than those calculated at  $\mathbf{P}=\mathbf{0}$  for the  $(\gamma, \text{pn})$  channel and stronger than those at  $\mathbf{P}=\mathbf{0}$  for the  $(\gamma, \text{pp})$  channel. In contrast,  $\Sigma$  calculations show a rather weak variation with  $\mathbf{P}$ , indicating that both  $\sigma_{\parallel}$  and  $\sigma_{\perp}$  have a similar  $\mathbf{P}$  dependence. Separate calculations were made for each combination of nucleon subshells ( $1p_{3/2}, 1p_{1/2}$  and  $1s_{1/2}$ ) and the results were averaged using relative spectroscopic factors obtained from an analysis of  $^{12}\text{C}(e, e'p)$  data<sup>2</sup>.

### 1.4 Results

The data presented below have been split into three  $E_m$  regions. Region I ( $E_m < 40$  MeV) corresponds to the ejection of nucleon pairs mainly from  $(1p)^2$  orbitals. Region II ( $40 < E_m < 70$  MeV) corresponds to emission from  $(1p)(1s)$  orbitals and Region III ( $70 < E_m < 120$  MeV) has substantial contributions from two-step processes<sup>13,14</sup>. Some of the  $(\vec{\gamma}, \text{pp})$  data shown below still require some small corrections and should therefore be regarded as preliminary, although this will not affect the general behaviour and trends reported.

The dependence of  $\Sigma$  on  $\mathbf{P}_{recoil}$  was investigated and found to be rather weak for both the  $^{12}\text{C}(\vec{\gamma}, \text{pn})$  and  $(\vec{\gamma}, \text{pp})$  reactions, for both  $E_m$  regions I and II<sup>2</sup>. For direct two-nucleon emission processes in the absence of significant Final State Interactions (FSI),  $\mathbf{P}_{recoil} = -\mathbf{P}$ . This implies that  $\Sigma$  does not have any strong  $\mathbf{P}$  dependence and hence, in order to improve the statistical accuracy of the data, all further analysis integrates the data over  $\mathbf{P}_{recoil}$ .

Some first results for the  $^{12}\text{C}(\vec{\gamma}, \text{pn})$  channel<sup>1</sup> have previously been reported. These showed that  $\Sigma$  for data corresponding to the predominant ejection of nucleons from  $(1p)^2$  orbitals is similar in magnitude to  $\Sigma$  for  $(\vec{\gamma}, \text{pn})$  reactions in other

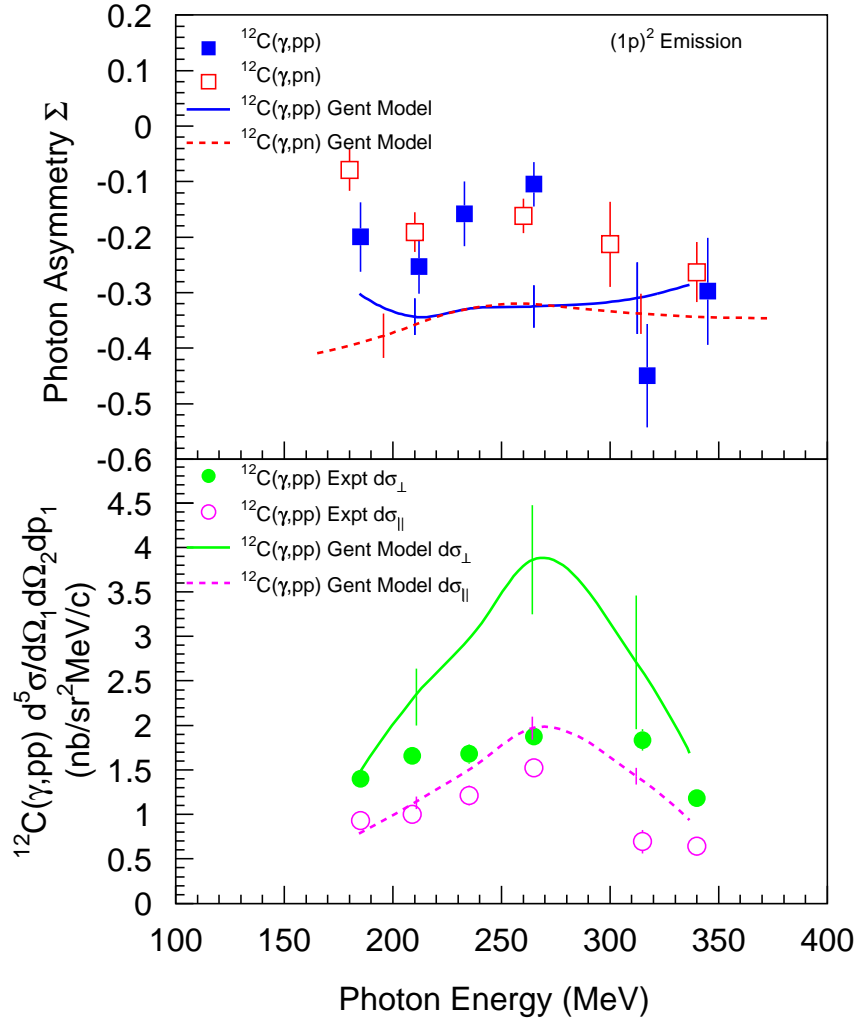


Fig. 1. Top Panel:  $\Sigma$  for  $^{12}\text{C}(\gamma, pp)$  (solid blue squares) and  $(\gamma, pn)$  (open red squares) for  $E_m < 40$  MeV, as a function of  $E_\gamma$ . Bottom panel:  $\sigma_{\parallel}$  (open pink circles) and  $\sigma_{\perp}$  (solid green circles) for  $^{12}\text{C}(\gamma, pp)$ . The lines are predictions from the Gent unfactorised model. The error bars on the calculations indicate the uncertainties due to the Monte Carlo sampling over the detector acceptances.

light nuclei<sup>15,16,17</sup>, although some of these include a rather wide range of  $E_m$ . The data also showed a small but systematic reduction in the magnitude of  $\Sigma$  compared to the  $^2\text{H}(\vec{\gamma}, pn)$  reaction. The  $\Sigma$  data for the ejection of nucleons from  $(1p)(1s)$  orbitals have a similar magnitude to the  $(1p)^2$  data although their photon energy dependence appears to be different.

Fig. 1 (top) shows a comparison of  $\Sigma$  for the  $^{12}\text{C}(\vec{\gamma}, pp)$  and  $(\vec{\gamma}, pn)$  reactions for  $E_m$  region I.  $\Sigma$  for both reactions is negative with the  $(\vec{\gamma}, pp)$  data having,

on average, a slightly larger magnitude than the  $^{12}\text{C}(\vec{\gamma},\text{pn})$  data. The  $^{16}\text{O}$  data from LEGS<sup>17</sup> also showed the  $(\vec{\gamma},\text{pp})$  asymmetry to be larger in magnitude than  $(\vec{\gamma},\text{pn})$ , although the effect observed in  $^{16}\text{O}$  is stronger than in  $^{12}\text{C}$ . The fact that the  $(\vec{\gamma},\text{pp})$  asymmetry has a larger magnitude than the  $(\vec{\gamma},\text{pn})$  asymmetry, in both nuclei, indicates that the  $(\gamma,\text{pp})$  reaction has a distinct mechanism and provides some further evidence to refute the suggestion that the  $(\gamma,\text{pp})$  reaction has a large contribution from initial  $(\gamma,\text{pn})$  processes followed by charge exchange FSI.

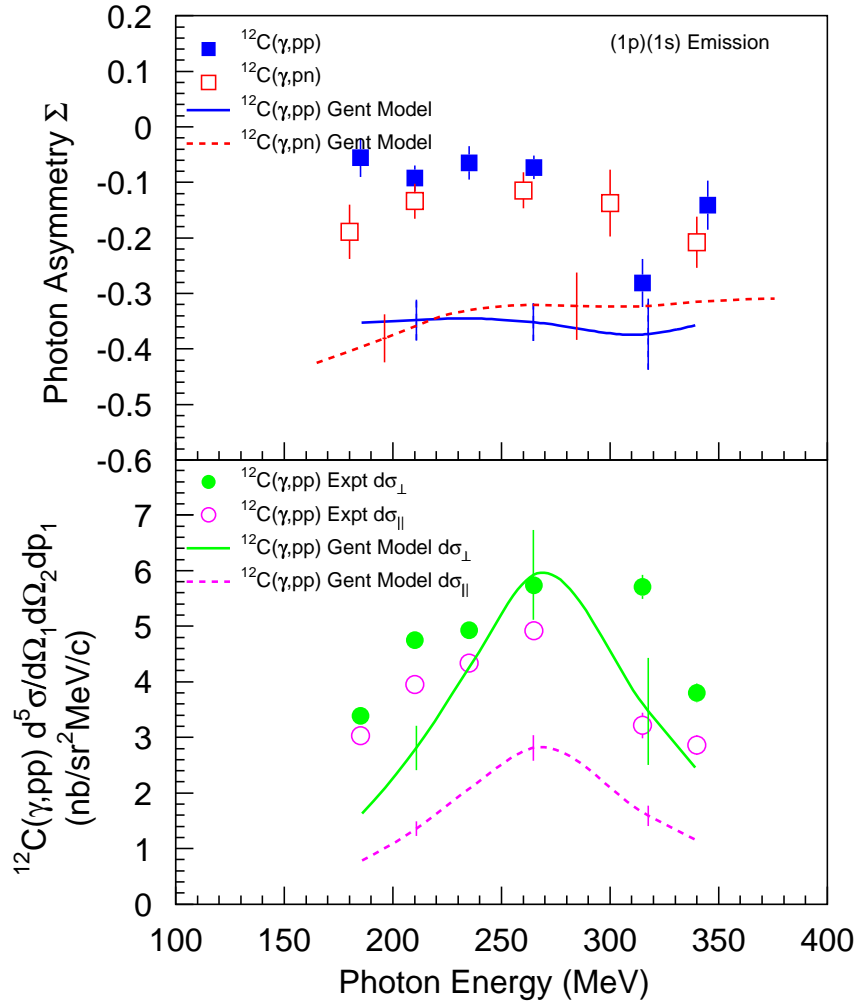


Fig. 2. As Fig. 1 for  $40 < E_m < 70$  MeV.

The comparison of the Gent model calculations with the  $\Sigma$  data is poor. As both reactions are dominated by  $\Delta$ -currents in this photon energy region the data suggest that the model requires a better description of the  $\Delta$ . The bottom panel shows data for the separate  $\sigma_{\parallel}$  and  $\sigma_{\perp}$  differential cross sections for the  $(\vec{\gamma},\text{pp})$

reaction. The calculations for  $\sigma_{\parallel}$  are in reasonable agreement with the experimental data whereas those for  $\sigma_{\perp}$  greatly overestimate the data in the  $\Delta$ -resonance region.

Fig. 2 shows a similar plot for data from  $E_m$  region II.  $\Sigma$  for the  $(\vec{\gamma}, pp)$  reaction has a slightly smaller magnitude than the  $^{12}\text{C}(\vec{\gamma}, pn)$  reaction. This change in behaviour was not expected. Although some contribution from FSI in this region might be expected to reduce the magnitude of  $\Sigma$  this may not be sufficient to explain the apparent quenching of the  $(\vec{\gamma}, pp)$  asymmetry. The Gent model calculations for both channels are similar to each other, but are a factor of  $\sim 2$  larger in magnitude than the data. Again the bottom panel shows  $\sigma_{\parallel}$  and  $\sigma_{\perp}$  for the  $(\vec{\gamma}, pp)$  reaction. For this  $E_m$  region the calculations for  $\sigma_{\perp}$  are much closer to the data than those for  $\sigma_{\parallel}$ .

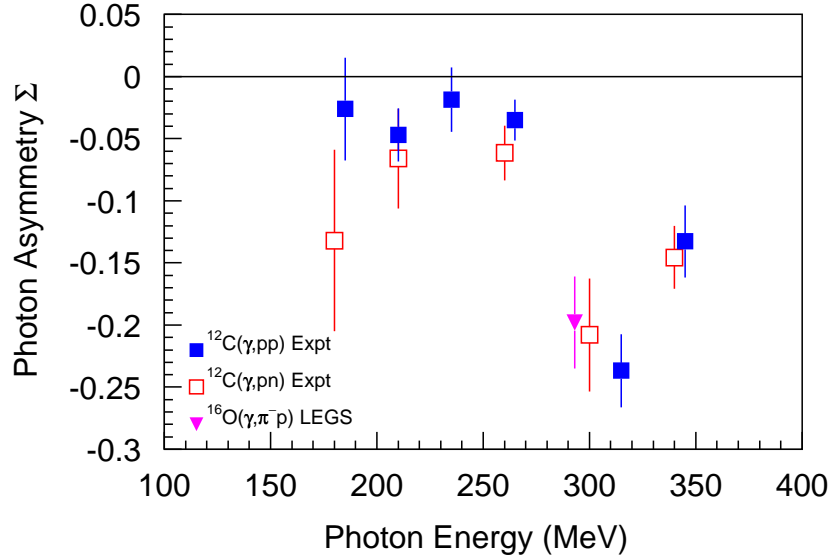


Fig. 3.  $\Sigma$  for  $^{12}\text{C}(\gamma, pp)$  (solid blue squares) and  $(\gamma, pn)$  (open red squares) for  $70 < E_m < 120$  MeV, compared with  $\Sigma$  for the LEGS  $^{16}\text{O}(\gamma, \pi^- p)$  reaction (solid pink triangle), as a function of  $E_\gamma$ .

Fig. 3 shows  $\Sigma$  for  $E_m$  region III for both reaction channels, together with data for the  $^{16}\text{O}(\vec{\gamma}, \pi^- p)$  reaction<sup>18</sup>.  $\Sigma$  for both two-nucleon emission channels is very similar. It has small magnitude for  $E_\gamma < 250$  MeV, but has a larger magnitude at higher photon energies. For both reaction channels this  $E_m$  region is dominated by two-step processes, the most important of which is initial pion production followed by pion reabsorption<sup>13,14</sup>. This process has been shown to become particularly strong at  $E_\gamma > 250$  MeV<sup>13</sup>.

Pion production on the proton has large asymmetry values:  $\Sigma \sim -0.35$  for

$p(\vec{\gamma}, \pi^+)n$  and  $\Sigma \sim -0.45$  for  $p(\vec{\gamma}, \pi^0)p$  at  $E_\gamma \sim 300$  MeV<sup>19</sup>.  $\pi^-$  production in  $^{16}\text{O}$  also has a reasonably strong  $\Sigma \sim -0.2$ <sup>18</sup>. This may derive from quasifree  $\pi^-$  production on bound neutrons, although the asymmetry of the quasifree pion production process is likely to be reduced somewhat by Fermi smearing in  $^{16}\text{O}$ . In photo-induced two-nucleon emission a similar transfer of photon asymmetry from an initial quasifree pion to the final nucleon pair may be possible since the  $\pi^+$  absorption cross section on the deuteron is largest at forward-backward nucleon angles<sup>20</sup>. However detailed models are required before this suggestion can be substantiated.

## 1.5 Summary

Section 1 of this paper reports the first polarised photon measurements of  $^{12}\text{C}(\vec{\gamma}, pp)$  and  $(\vec{\gamma}, pn)$  reactions.  $\Sigma$ ,  $\sigma_{\parallel}$  and  $\sigma_{\perp}$  have been measured in three separate missing energy regions for photon energies spanning the  $\Delta$ -resonance. Clear differences are observed between the various missing energy regions and between the two reaction channels. The data have been compared to the latest available theoretical models, averaged over the experimental detector acceptances. Unfortunately these do not yet give an adequate description of the data and this has precluded a more detailed interpretation of the contributing reaction mechanisms.

The present measurements have raised some interesting questions and have already provided important tests for reaction models. However there is a clear need for further experiments to a) obtain data with better statistical accuracy, b) obtain information on specific states in the residual nucleus using high resolution detectors, c) cover a wider range of photon energies, especially away from the  $\Delta$ -resonance, and d) to investigate differences between nuclei.

## 2 Short Range Effects in the $^{12}\text{C}(\gamma, NN)$ Reaction

### 2.1 Introduction

This section describes a proposed experiment<sup>21</sup> to study nucleon-nucleon SRC by measuring the  $^{12}\text{C}(\gamma, pp)$  and  $(\gamma, pn)$  reaction cross sections at photon energies above the  $\Delta$ -resonance in kinematics close to the photon beam line. The experiment was approved by the Mainz/Bonn PAC in the Autumn of 1998 and will take place in the Mainz A2 Hall when scheduling allows.

### 2.2 Kinematic Regions sensitive to SRC

While previous  $(\gamma, NN)$  work has greatly improved our understanding of the contributing reaction mechanisms it has not explored kinematic regions which are sensitive to SRC. In particular, previous experiments have concentrated on pho-

ton energies below 400 MeV which are dominated by long range MEC and  $\Delta$ -production. The proposed experiment will explore forward-backward nucleon pair production and regions of high initial pair momenta at photon energies above the  $\Delta$ -resonance. Evidence suggesting these regions are worth detailed study comes from the small amount of experimental work which has been carried out at high photon energies<sup>22</sup> and from theoretical calculations of two-nucleon emission.

One previous experiment measured  $^{12}\text{C}(\gamma,\text{pn})$  and  $(\gamma,\text{pp})$  reactions in regions of extreme kinematics, well away from the usual “back-to-back” quasideuteron regime<sup>22</sup>. This experiment provided a small amount of data at photon energies above the  $\Delta$ -resonance and also sampled very large values of  $\mathbf{P}$ , the initial momentum of the participating pair. Events corresponding to the ejection of nucleon pairs from  $(1p)^2$  orbitals were selected by cutting on  $E_m < 40$  MeV. The excitation function for the  $^{12}\text{C}(\gamma,\text{pn})$   $(1p)^2$  emission data was observed to fall rapidly above the  $\Delta$ -resonance before showing a small increase for  $E_\gamma > 500$  MeV. A comparison with the shape of the two-body  $^2\text{H}(\gamma,\text{pn})$  excitation function showed that  $^{12}\text{C}$  had relatively more strength at very high photon energies. As high  $E_\gamma$  correspond kinematically to large relative momenta  $\mathbf{P}_{rel}$  of the interacting pair<sup>23</sup>, strength in this region may arise from SRC producing violent nucleon-nucleon collisions. In addition to showing that the  $^{12}\text{C}(\gamma,\text{pn})$  cross section is large enough to permit a reasonable measurement above the  $\Delta$ -resonance the comparison provides some tentative evidence to suggest that SRC may be somewhat stronger in  $^{12}\text{C}$  than in deuterium.

Further information on the sensitivity of  $(\gamma,\text{NN})$  reactions to SRC comes from theoretical calculations of the two-nucleon emission process. Calculations for the  $(\gamma,\text{pp})$  channel were carried out using a factorised model developed by the Gent group<sup>5</sup>. The factorised approach is known to overestimate the effects of central SRC and to underestimate  $\Delta$ -currents. In addition the calculations presented extrapolate the reaction cross sections to higher photon energies than the models were initially designed to address. Nevertheless, these calculations may give a useful indication of the most promising kinematic regions to study.

This model shows the different kinematic dependences of the contributions from central SRC and from  $\Delta$ -currents. Pions created from the decay of the  $\Delta$ -resonance are predominantly emitted in a direction orthogonal to the direction of the photon beam. Contributions to the  $(\gamma,\text{pp})$  channel from the reabsorption of these pions are therefore small at extreme forward and backward angles. In contrast, the effects due to SRC are maximised at small angles. They also increase with photon energy, again in contrast to the  $\Delta$ -currents which decrease rapidly in importance above 400 MeV.

Fig. 4 shows the photon energy dependence of the  $(\gamma,\text{pp})$  cross section calculated for a range of reasonable central correlation functions, for various polar angles in the centre-of-momentum frame of the photon and the interacting pair. The SRC



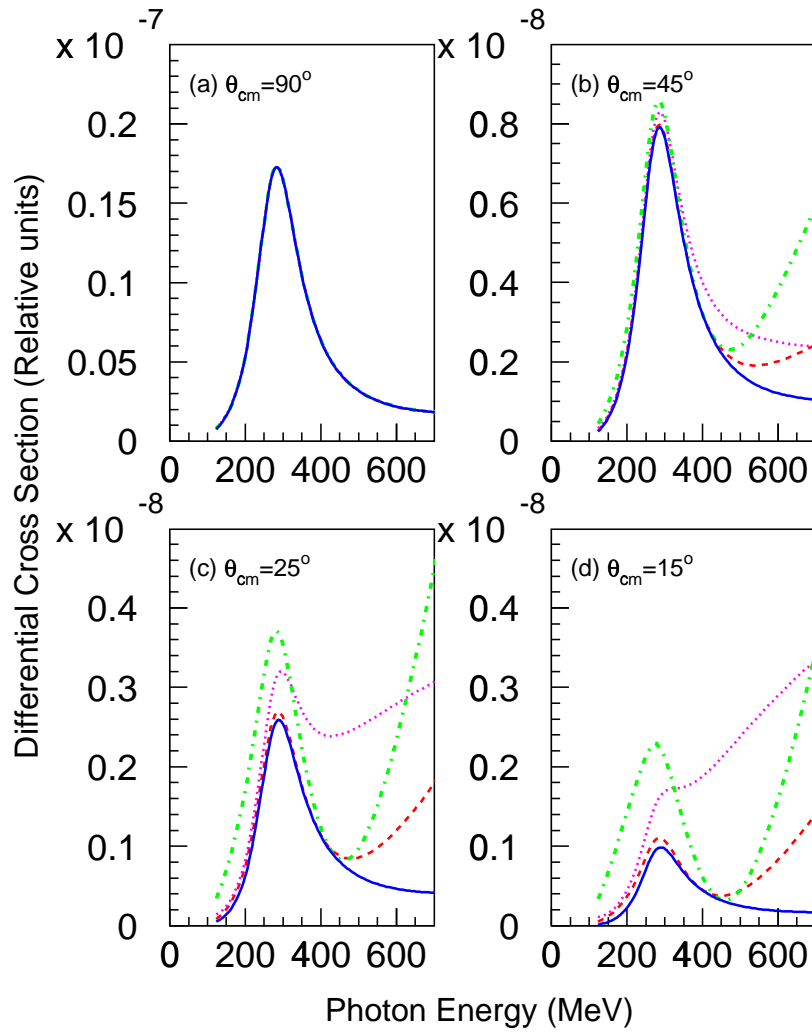


Fig. 4. Calculated  $E_\gamma$  dependence of the  $(\gamma, pp)$  cross section using the factorised Gent model, for events with  $P=300$  MeV/c. The solid blue line shows the  $\Delta$  term on its own. The red dashed line uses a VMC calculation of SRC. The pink dotted line uses a FHNC calculation and the green dot-dashed uses the GD prediction. Panel (a) corresponds to symmetric kinematics ( $\theta_{CM} = 90^\circ$ ). Panels (b), (c) and (d) correspond to  $\theta_{CM}=45^\circ$ ,  $25^\circ$  and  $15^\circ$ .

effects become more important as the photon energy increases and above 500 MeV SRC provide a strong enhancement of the cross section at extreme forward and backward angles. The large differences between the  $\Delta$ -current contributions and SRC are such that the experiment will be readily able to identify whether or not SRC contribute significantly to the  $(\gamma, pp)$  channel. Indeed, the data at forward-

backward angles should be able to distinguish at least some of these different possible SRC. It is also interesting to note that the sensitivity to SRC vanishes in symmetric kinematics where  $\theta_{cm} = 90^\circ$  and this fact may be used to establish the strength of the competing  $\Delta$ -current contribution.

In (e,e'pp) experiments<sup>24</sup> the corresponding “super-parallel” kinematics have been exploited to reduce the number of contributing structure functions. These complementary reactions are predominantly sensitive to longitudinal interactions and while the use of magnetic spectrometers permits measurements in precise kinematics they have the disadvantage of sampling very small regions of phase space and suffer from relatively poor statistical accuracy. Previous electron scattering experiments have also concentrated on momentum transfers below the  $\Delta$ -resonance whereas the present experiment will probe short distances with momentum transfers above the  $\Delta$ -resonance.

From isospin considerations it is generally expected that tensor correlations will be more important in the ( $\gamma$ ,pn) channel than central SRC and this is confirmed by recent nuclear matter (e,e'NN) calculations<sup>25</sup> which suggest that tensor correlations are a factor of  $\sim 7$  stronger than central correlations. These calculations also show that the contribution from SRC to the transverse response function increases with photon momentum. This is true for both channels, for kinematics where the two outgoing nucleons have unequal energies (*i.e.* away from symmetric  $cm$  angles), but the photon momentum dependence is considerably stronger in the pp channel. These findings re-iterate that high energies and non-symmetric kinematics provide the best location for studying SRC effects.

While the proposed experiment aims primarily to measure the ( $\gamma$ ,pp) cross section it will also make a good measurement of the ( $\gamma$ ,pn) cross section in the same kinematic regions, providing data against which models of both reactions can be tested.

Fig. 5 shows the initial pair momentum spectra obtained in our previous  $^{12}\text{C}(\gamma,\text{pn})$  wide-phase-space experiment<sup>22</sup> which sampled kinematics away from the standard quasideuteron “back-to-back” kinematics. In particular, this experiment was moderately sensitive to regions of very large pair momentum. The data have been divided by the initial pair momentum distribution  $F(P)$ , calculated using Harmonic Oscillator nucleon wavefunctions, to emphasise differences from the standard mean-field predictions. There is a systematic enhancement at pair momenta above 400 MeV/c for data from all three kinematic regions sampled. It is expected that this may be due either to SRC, or to soft FSI which do not significantly change the energies of the outgoing nucleons. We also show a calculation by Orlandini and Sarra<sup>26</sup> which includes the effects of SRC in the case of  $^{16}\text{O}$ . This gives a reasonable description of most of the excess strength. It is clear that better quality data at large recoil momenta would provide a very useful test of theoretical models incorporating both SRC and FSI.

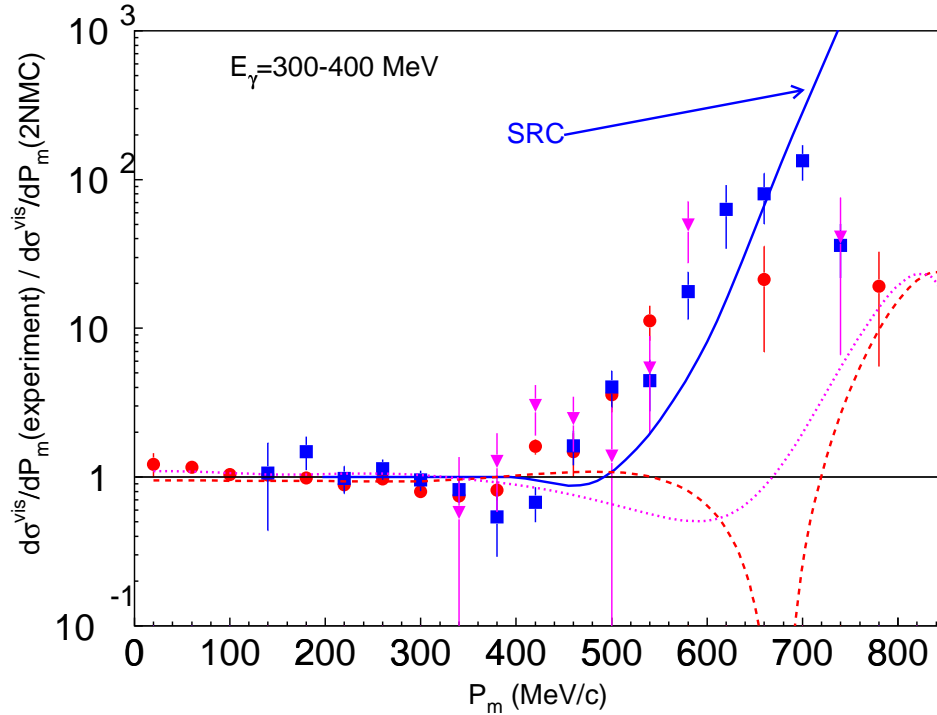


Fig. 5. Ratio of  $^{12}\text{C}(\gamma, pn)$  initial pair momentum data to the calculated pair momentum distribution  $F(P)$  at  $E_\gamma=300\text{-}400$  MeV for  $E_m \leq 40$  MeV. The red circles correspond to “back-to-back” quasideuteron kinematics. The blue squares and pink triangles represent data with successively larger opening angles<sup>22</sup>. A calculation, including the effects of SRC, for  $^{16}\text{O}$  by Orlandini and Sarra<sup>26</sup> is shown by the solid blue line. The red dashed (pink dotted) lines show the deviation from the harmonic oscillator  $F(P)$  distribution when using more realistic Hartree-Fock (Woods-Saxon) wavefunctions.

### 2.3 Experiment

The experiment will use the Glasgow tagged photon spectrometer<sup>6</sup> at the Mainz microtron MAMI<sup>7</sup> to measure the energy and flux of incident photons. Protons and neutrons will be detected using the PiP<sup>9</sup> and TOF<sup>10</sup> detector arrays as shown in Fig. 6. TOF stands ABC and DEF will be placed  $\sim 6\text{m}$  from the target as close in angle to the photon beam line as counting rates will allow. At  $E_\gamma \sim 500$  MeV forward going particles will have average kinetic energies of  $\sim 370$  MeV. By stacking three TOF stands behind each other it will be possible to detect protons of energies up to  $\sim 450$  MeV, providing good sensitivity to low  $E_m$  events at high  $E_\gamma$ . Using three layers will also increase the neutron detection efficiency to  $\sim 0.15$ . Correlated particles at backward angles will be detected in TOF stands IJ and KL, covering  $120^\circ\text{-}170^\circ$  at a distance of  $\sim 2\text{m}$ . The overall energy resolution of the experiment is expected to be better than 12 MeV which is sufficient to separate the initial shells of the emitted nucleons.

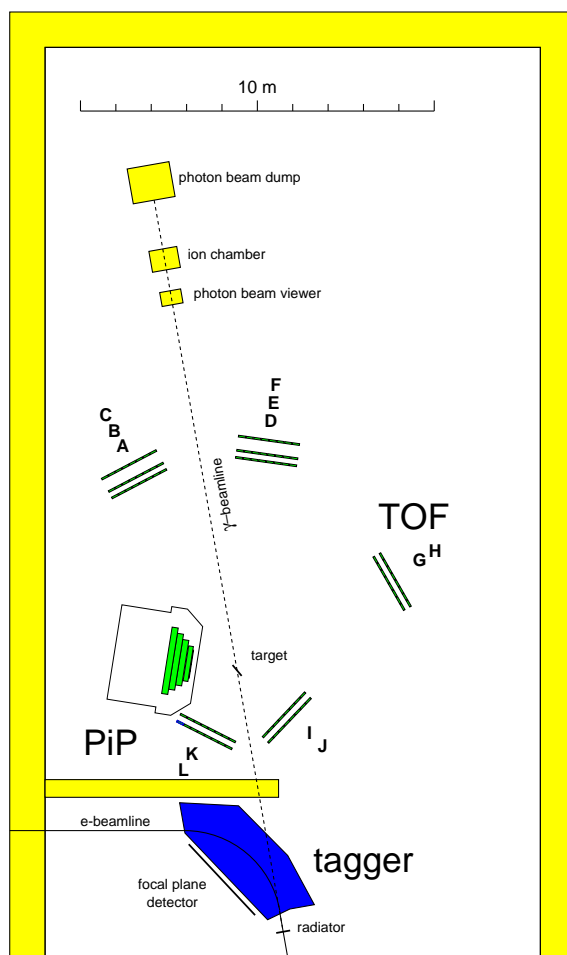


Fig. 6. Proposed Detector Layout

As calculations have shown that there is no sensitivity to SRC in symmetric coplanar kinematics, PiP and the TOF stands GH, placed symmetrically on opposite sides of the photon beam, will provide a reference datum point to which the theoretical shape of the differential cross section due to the  $\Delta$ -current can be scaled.

Data at high values of missing momenta will be obtained from coincidences between TOF stands ABC and KL, DEF and GH, and ABC and PiP.

## 2.4 Summary

The experiment will investigate ( $\gamma$ ,NN) reactions in regions as close to the photon beam direction as experimentally practical and in regions of very large missing momenta for photon energies above the  $\Delta$ -resonance. The experiment will concentrate on the ( $\gamma$ ,pp) channel, where the effects due to SRC are expected to be easier to disentangle, but will also simultaneously measure the ( $\gamma$ ,pn) cross section in the same kinematic regions. While two-proton emission has previously been studied by the complementary electron scattering reaction in super-parallel kinematics, it has not been studied in similar kinematics in photonuclear experiments and proton-neutron emission has not yet been studied by either reaction in these kinematic regions.

## Acknowledgements

Thanks are due to Dr. J. Ryckebusch, University of Gent, for allowing the use of his photonuclear two-nucleon knockout codes in the analysis of the polarised photon data and in determining kinematic regions sensitive to SRC. This work was supported by the UK EPSRC, the British Council, the DFG (SFB201 and Mu750/3), DAAD (313ARC-IX-95/41 & 313ARC-XII-98/32) and NATO (CRG 970268).

## References

1. S. Franczuk *et al.*, Phys. Lett. **B450** (1999) 332
2. C.J.Y. Powrie *et al.*, to be published
3. S. Boffi, C Giusti, F.D. Pacati and M. Radici, Electromagnetic Response of Atomic Nuclei, Oxford University Press (1996);  
S. Boffi *et al.*, Nucl. Phys. **A564** (1993) 473
4. C. Giusti, contribution to this workshop;  
C. Giusti and F.D. Pacati, Nucl. Phys. **A641** (1998) 297 ;  
C. Giusti *et al.*, Nucl. Phys. **A546** (1992) 607
5. J. Ryckebusch, contribution to this workshop;  
J. Ryckebusch *et al.*, Phys. Rev. **C57** (1998) 1319 ;  
J. Ryckebusch *et al.*, Phys. Lett. **B291** (1992) 213 ;  
L. Machenil *et al.*, Phys. Lett. **B316** (1993) 117 ;  
J. Ryckebusch *et al.*, Nucl. Phys. **A580** (1994) 551
6. S.J. Hall *et al.*, Nucl. Instr. Meth. **A368** (1996) 698 ;  
I. Anthony *et al.*, Nucl. Instr. Meth. **A301** (1991) 230
7. H. Herminghaus, Proc. Linear Accelerator Conf., Albuquerque, USA (1990);  
T. Walcher, Prog. Part. Nucl. Phys. **24** (1990) 479
8. F.A. Natter, contribution to this workshop;  
F.A. Natter *et al.*, to be published

9. I.J.D. MacGregor *et al.*, Nucl. Instr. Meth. **A382** (1996) 479
10. P. Grabmayr *et al.*, Nucl. Instr. Meth. **A402** (1998) 85
11. D.G. Ireland, contribution to this workshop;  
D.G. Ireland, I.J.D. MacGregor and J. Ryckebusch, Phys. Rev. **C59** (1999) 3297
12. C.C. Gearhart, Ph.D. Thesis, University of Washington (1994);  
W. Dickhoff, private communication
13. T. Lamparter *et al.*, Z. Phys. **A355** (1996) 1
14. P.D. Harty *et al.*, Phys. Lett. **B380** (1996) 247 ;  
P.D. Harty *et al.*, Phys. Rev. **C57** (1998) 123
15. D.J. Tedeschi *et al.*, Phys. Rev. Lett. **73** (1994) 408
16. F.V. Adamian *et al.*, J. Phys. **G17** (1991) 1657
17. R. Lindgren, contribution to this workshop;  
R. Lindgren *et al.*, to be published
18. K. Hicks *et al.*, Phys. Rev. **C55** (1997) R12
19. F.A. Berends *et al.*, Nucl. Phys. **B4** (1967) 54
20. H.J. Weyer, Physics Reports **195** (1990) 295
21. I.J.D. MacGregor *et al.*, Mainz/Bonn PAC proposal A2/2-98 (1998)
22. D.P. Watts, contribution to this workshop;  
D.P. Watts *et al.*, to be published
23. P. Grabmayr *et al.*, Proc. 14th Int. Conf. Particles and Nuclei, Williamsburg 1997, Ed. C.E. Carlson and J.J. Domingo, World Scientific Publishing 1997, ISBN 981-02-3003-6, pp. 296-297
24. G. Rosner, contribution to this workshop;  
K.I. Blomqvist *et al.*, Phys. Lett. **B421** (1998) 71 ;  
C.J.G. Onderwater *et al.*, Phys. Rev. Lett. **81** (1998) 2213
25. H. Müther, contribution to this workshop;  
D. Knödler and H. Müther, to be published
26. G. Orlandini and L. Sarra, Proc. 2nd Workshop on Electromagnetically Induced Two-Nucleon Emission, Gent 1995, Ed. J. Ryckebusch and M. Waroquier, pp. 1-10